A SYNTHESIZED APPROACH FOR PREDICTING LIQUEFACTION AND RESULTING DISPLACEMENTS

Michael H BEATY[1] And Peter M BYRNE[2]

SUMMARY

A mechanics-based approach is presented for assessing post-liquefaction displacements of geotechnical structures. The approach is derived from total stress procedures in common use, with two major advantages: (1) the triggering and post-liquefaction response have been synthesized into one analysis, and (2) the modelling of post-liquefaction element behaviour is greatly improved. Analyses are performed in the time domain, allowing the imposed earthquake motion to affect both the triggering and post-liquefaction deformations. General two-dimensional structures may be evaluated using finite-difference techniques. The approach is presented through the simulation of two case histories: the response of the Upper and Lower San Fernando dams to the 1971 San Fernando earthquake. The magnitude and pattern of the predicted displacements are shown to be in good agreement with the measured values.

INTRODUCTION

Two questions must be answered in most liquefaction assessments: (1) will liquefaction occur in significant zones? and (2) what displacements will occur? Displacements are often small when liquefaction does not occur and may be estimated using pre-liquefaction properties. A large drop in stiffness and strength typically occurs with liquefaction, and damaging displacements may result if the liquefied zones are of sufficient extent. Two approaches are available to estimate these displacements: empirical equations and mechanics-based analyses.

Empirical relationships are valuable as they directly include the intangible aspects of field response. They are derived from field observations, are often limited to specific topographic and material conditions, and may be impractical for evaluating two-dimensional effects. Mechanics-based methods approximate soil behaviour using numerical models. These models attempt to capture the physics of soil response, although their success is limited by inherent simplifications. These methods require some knowledge of soil properties, such as stiffness and strength. Mechanics-based approaches vary in complexity from equivalent-linear methods [Idriss and Sun, 1992] to advanced effective stress models [Beaty and Byrne, 1998; Finn et al., 1986]. The accepted state of practice in Canada and the United States is often a three-phase total stress procedure:

- Triggering evaluation: Zones of liquefaction are predicted by comparing estimates of cyclic shear stress to the anticipated resistance to liquefaction. Equivalent linear techniques are often used. Triggering resistance is frequently based on empirical correlation and in-situ tests [Youd and Idriss, 1998].

- Flow slide evaluation: If significant zones of liquefaction are predicted, the potential for a flow slide is evaluated using limit equilibrium techniques. The susceptibility to large deformations is found by assigning residual strengths to the liquefied zones and appropriate undrained strengths to non-liquefied material. If the safety factor is less than or near 1, large deformations are assumed.

- Displacement evaluation: Large but limited displacements may occur even if the structure has sufficient strength to maintain overall stability. These displacements accumulate during the earthquake and are a

---

[1] University of British Columbia, Civil Engineering Department, Vancouver, Canada (Email: beaty@civil.ubc.ca)
[2] University of British Columbia, Civil Engineering Department, Vancouver, Canada (Email: pmb@civil.ubc.ca)

direct result of the continuing inertia loading. Techniques for estimating these displacements are often based on Newmark [1965] and model the displacing soil as a rigid block translating on a plane.

Current practice has many advantages, including wide experience and the relative simplicity of procedure and input. There are also drawbacks including the simple evaluation of triggering, the crude modelling of post-liquefaction mechanics, and the disjointed nature of the three-phase procedure. The approach presented below attempts to capitalize on the experience and understanding of current practice, while synthesizing the components of a total stress evaluation into a more coherent, rational method.

SYNTHESIZED APPROACH

The framework of the synthesized approach is the numerical solution technique. A finite-difference continuum model is used, although the approach can be adapted to other methods such as finite element. General two-dimensional structures are discretized into elements, masses are lumped at nodal points, and constitutive relationships and properties are assigned. An explicit solution scheme is used where the dynamic equations of equilibrium are satisfied for each mass at every timestep. This allows changes in the material stiffness, strength, or stress of an element to be rationally considered: each element strains dynamically in response to out-of-balance forces. This scheme requires small timesteps, often less than 0.0001 seconds, but easily models non-linear and large strain response. The commercial code FLAC is used to perform the calculations [Itasca, 1998].
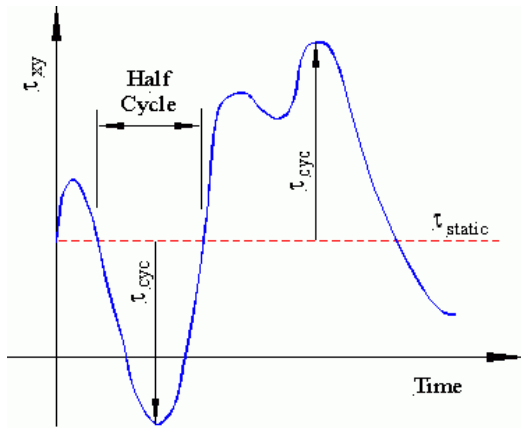
Pre-Liquefaction

The analysis prior to liquefaction is similar to the equivalent linear method. A linear elastic-plastic constitutive model is used in combination with Rayleigh stiffness-proportional viscous damping. Elastic moduli are estimated from the maximum shear modulus, G_{max}, and a modulus reduction factor, MRF. But unlike equivalent linear methods, the synthesized approach is not iterative. Appropriate values of MRF and damping are selected prior to the analysis. Suitable values of undrained strength, S_u, are also assigned. Changes in pore pressure prior to liquefaction are not directly included, but can be approximated through a reduction in stiffness.
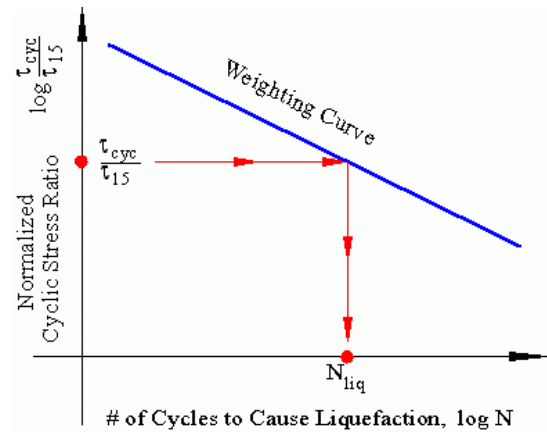
Triggering of Liquefaction

Triggering of liquefaction is evaluated by tracking the dynamic shear stress on the horizontal plane, τ_{xy}, within each element. The cyclic pulse, τ_{cyc}, is computed at every timestep and is defined as $\tau_{cyc} = |\tau_{xy} - \tau_{static}|$, where τ_{static} is the τ_{xy} that existed prior to the earthquake. The irregular stress history is interpreted as a succession of half cycles, with the contribution of each half cycle determined by its maximum value of τ_{cyc}. This definition of cyclic loading is shown schematically in Figure 1.

A cumulative damage technique combines the effect of each half cycle. This approach converts the non-uniform τ_{cyc} history into an equivalent series of uniform stress cycles. The amplitude of the uniform history is arbitrarily set to τ_{15}, which is the value of τ_{cyc} required to cause liquefaction in 15 cycles. This transformation uses the cyclic strength curve as a weighting curve as shown in Figure 2 and described below. The approach is similar to work developed at the University of California at Berkeley [Lee and Chan, 1972].

1.   For each half cycle, use weighting curve to find N_{liq}, the number of uniform cycles of τ_{cyc} required to cause liquefaction.

2.   Multiply N_{liq} by 2 to find the number of half cycles of τ_{cyc} needed to cause liquefaction.

3.   Compute relative contribution of current half cycle to liquefaction: $1/(2 \times N_{liq})$.

4.   Compute equivalent number of cycles based on 15 cycles to liquefaction: $N_{eq} = 15/(2 \times N_{liq})$.

5.   Sum the effect of each half cycle, ΣN_{eq}. Liquefaction is triggered when $\Sigma N_{eq} \geq 15$.

Figure 1: Half Cycle and τ_{cyc}


Figure 2: Weighting Curve

An idealized stress-strain curve showing the onset of liquefaction is given in Figure 3. The synthesized method attempts to capture this behaviour by continuously evaluating τ_{cyc} rather than just peak values. Triggering is assumed when the current value of τ_{cyc} is sufficient to bring ΣN_{eq} to 15 at the end of the next half cycle. This causes triggering to begin when the element is under shear stress, rather than at a stress reversal. The direction of τ_{xy} is also considered as it is often more likely to initiate liquefaction when the cyclic pulse and the static bias are in the same direction.

Since the triggering of each element is evaluated separately, liquefaction first occurs in the most susceptible areas and then spreads with further dynamic loading in a realistic manner. The effects of progressive liquefaction, including load shedding and base isolation, are rationally considered.

Post-Liquefaction

A reduced stiffness and a residual strength is specified when liquefaction is triggered in an element. The constitutive model is also modified so that unloading occurs along a stiffer path than loading, as shown in Figure 4. This bilinear model permits the accumulation of displacement with each cycle while still maintaining a simple elastic-plastic formulation. Due to the large hysteretic damping component, the viscous damping coefficients in the liquefied elements are also reduced.

Anisotropy is incorporated by making the strength a function of the major principal stress direction. Residual strengths are specified for known stress paths, usually corresponding to compression and simple shear. An interpolation function derived from hollow cylinder test results is then used to vary the strength with principal stress direction. The importance of anisotropy during monotonic loading has been well demonstrated by hollow cylinder torsion tests [Vaid and Sivathayalan, 1999]. Undrained strengths of water-pluviated sand can vary by factors of 3 to 5 or more depending on the stress path.
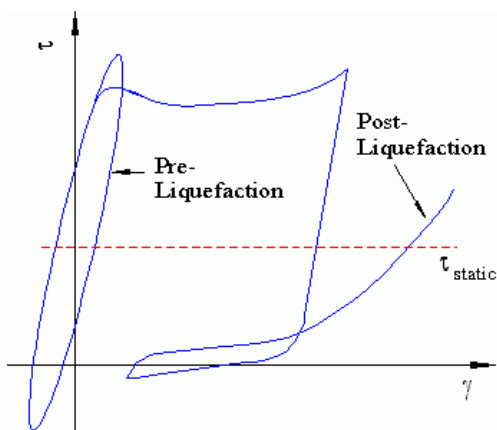
Figure 3: Idealized Stress-Strain Behaviour
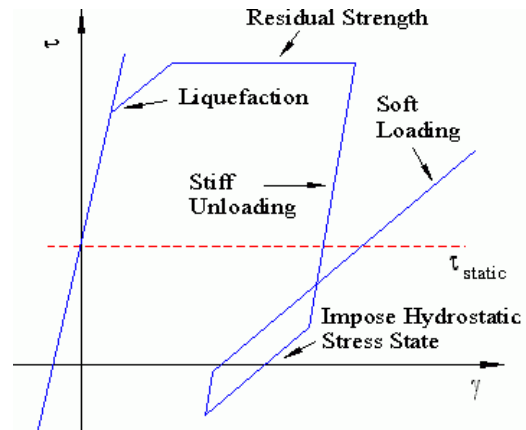
Figure 4: Synthesized Approach Model

Another feature of liquefied behaviour is the occurrence of high pore pressure and loss of effective stress at shear stress reversals. This is simulated by imposing a hydrostatic stress state whenever a liquefied element experiences a shear stress reversal. The lateral total stresses are set equal to the vertical stress and the horizontal shear stress is removed: $\sigma_{xx} = \sigma_{yy}$, $\sigma_{zz} = \sigma_{yy}$, and $\tau_{xy} = 0$. Imposing these stresses momentarily removes all shear stress from the element, as is the case when the excess pore pressure ratio, r_u, equals 100%.

The simple bilinear model shown on Figure 4 causes the shear stress to increase quickly after a stress reversal. This representation is adequate when strains accumulate primarily in one direction, such as may occur for elements with a pronounced static bias. A softened loading modulus can also be imposed immediately after a stress reversal to more accurately model symmetric loading.

The approach described above assumes a rapid transition into liquefied behaviour. This may not always occur, especially for denser materials. Contrary to intuition, assuming a quick transition into liquefied behaviour may lead to an underprediction of the displacements. Early liquefaction can introduce base isolation effects that limit the final extent of liquefaction. Such possibilities must be considered when evaluating analyses.

Comparison with Empirical Procedure

Empirical methods reflect a large database of observed behaviour and can be useful for verifying or calibrating a mechanics-based approach. Such an evaluation of sloping ground conditions has been made using the Bartlett and Youd [1995] empirical method. A detailed presentation of the analyses is provided by Beaty and Byrne [1999]. In summary, reasonable agreement was obtained between the two methods. The results indicate the importance of soil conditions below the liquefied soil, the direction of the applied base motion, and possibly the frequency content of the earthquake.

SIMULATION OF THE SAN FERNANDO DAMS

The Lower and Upper San Fernando dams are located in southern California, roughly 30 kilometres north of downtown Los Angeles. The dams were built as part of the Los Angeles Aqueduct system, with construction beginning in 1912 for the lower dam and 1921 for the upper dam. Both dams were built using variations of the hydraulic fill method [Seed et al., 1973]. This method yielded a central clayey core with highly stratified shells consisting of sand, silty sand, and clay. The sandy layers have a representative fines content of about 25%.

The Lower San Fernando dam was about 44 metres in height, founded on up to 11 metres of alluvium, and originally had slopes of 2.5:1. A rolled fill berm with a 4.5:1 slope was added to the downstream face in 1940. This berm creates a 6-metre-wide bench at an elevation 15 metres below the crest. The upper dam was constructed on about 15 to 18 metres of alluvium overlying bedrock. The dam is approximately 21 metres high, although it was not constructed to its full intended height. Instead, a 5.5-metre-high rolled fill section was placed on the upstream portion of the hydraulic fill, leaving a 30.5-metre-wide bench on the downstream slope. This gives the dam a very wide profile for its height. The slopes of the dam are 2.5:1.

Observed Seismic Response

The San Fernando earthquake occurred on February 9, 1971, had an M_w of 6.6, and an epicentre about 11 km from the dams. Peak ground accelerations at the site were estimated to be around 0.6g. The response of the lower dam was dominated by the near catastrophic slide of the upstream face and crest. The 11 metres of freeboard prior to the earthquake were reduced to a fragile 1.5 metres. An extensive field investigation found that liquefaction of the fill near the base of the upstream shell was responsible for the slide [Seed et al., 1973]. The slide extended 45 to 60 metres into the reservoir. Large blocks of intact fill were transported by the liquefied soil. An evaluation of the crest seismoscope record indicates the slide occurred about 20 to 30 seconds after the earthquake shaking had stopped [Seed et al., 1988].

The performance of the upper dam was less dramatic. The crest and downstream berm moved 1.5 to 2 metres downstream, with the crest dropping up to one metre. Several longitudinal cracks ran the length of the upstream face near the reservoir level [Serff et al., 1976]. A 0.6-metre-high pressure ridge was also observed at the downstream toe. Tension cracks and evidence of compression failure were seen in the outlet conduit at the base of the embankment. Liquefaction was suggested by sand boils below the toe and increased water levels in the three standpipe piezometers. Water overflowed from two of the piezometers.

Description of FLAC Models and Input Properties

The FLAC models were based on representative sections developed by Seed et al. [1973] and are shown in Figure 5. Material properties were derived primarily from the laboratory and in-situ testing performed in 1973. The $(N_1)_{60}$ characterization was based on the work of Seed et al. [1988] for the lower dam and Harder et al. [1989] for the upper dam. Values of MRF and viscous damping were estimated by comparing SHAKE and FLAC analyses of representative columns. The input earthquake motion was the modified Pacoima dam record prepared by Seed et al. [1973] and scaled to 0.55g for the lower dam and 0.6g for the upper dam. Selected input properties are given in Table 1.

Cyclic triaxial testing has been performed on "undisturbed" samples from each dam [Seed et al., 1973; Seed et al., 1988]. Weighting curves for each dam were derived from these tests. A fines content correction for triggering was also estimated from the 1988 tests. Values of τ_{15} and K_σ were determined using the appropriate MCEER curves [Youd and Idriss, 1998]. K_α was assumed equal to unity.

Limit equilibrium analyses have been performed on both the upper dam [Harder et al., 1989] and the lower dam [Seed et al., 1988] to estimate values of residual strength. These were converted to S_r / σ'_{vo} values by dividing the S_r estimate with the average value of initial vertical effective stress within the significant liquefied material. The conversion produced S_r / σ'_{vo} values of 0.06 to 0.10 for the lower dam and 0.13 to 0.19 for the upper dam. The range estimated for the lower dam is quite low, especially when compared to the upper dam. The mixing of clean and silty fill materials as the slide moved into the reservoir may be one cause of these low strength values. The hydraulic fill of both dams is highly stratified, and mixing with an associated loss of strength is anticipated during these large strains. The strength range estimated for the lower dam is appropriate for the end of sliding, but the initial residual strength was likely higher. Using the trend shown by Byrne and Beaty [1999] and the strengths estimated for the upper dam, a modified S_r / σ'_{vo} value was developed for the lower dam analysis.

FLAC Analysis

The initial static analyses were performed using a hyperbolic model. The embankment was constructed in layers and the reservoir load was added. Once the grid reached equilibrium, the constitutive model was changed, dynamic properties were assigned, and the earthquake motion was applied to the base. Liquefaction was permitted throughout the saturated hydraulic fill zone, but not in the other embankment zones or the foundation.

Results for Lower San Fernando Dam

Two features distinguish the actual response of the Lower San Fernando dam: (1) limited displacements during the earthquake, and (2) a near catastrophic failure of the upstream slope following the earthquake. Figure 6a
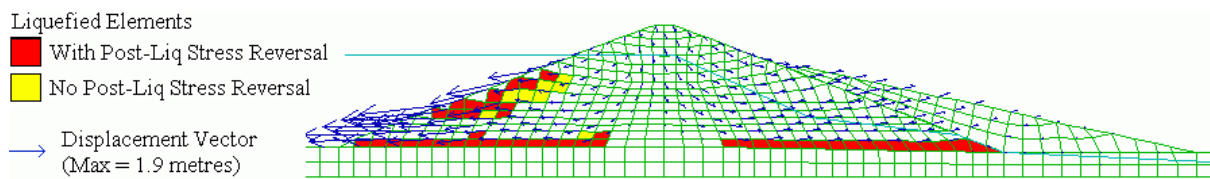

a) **Lower San Fernando Dam**

b) **Upper San Fernando Dam**
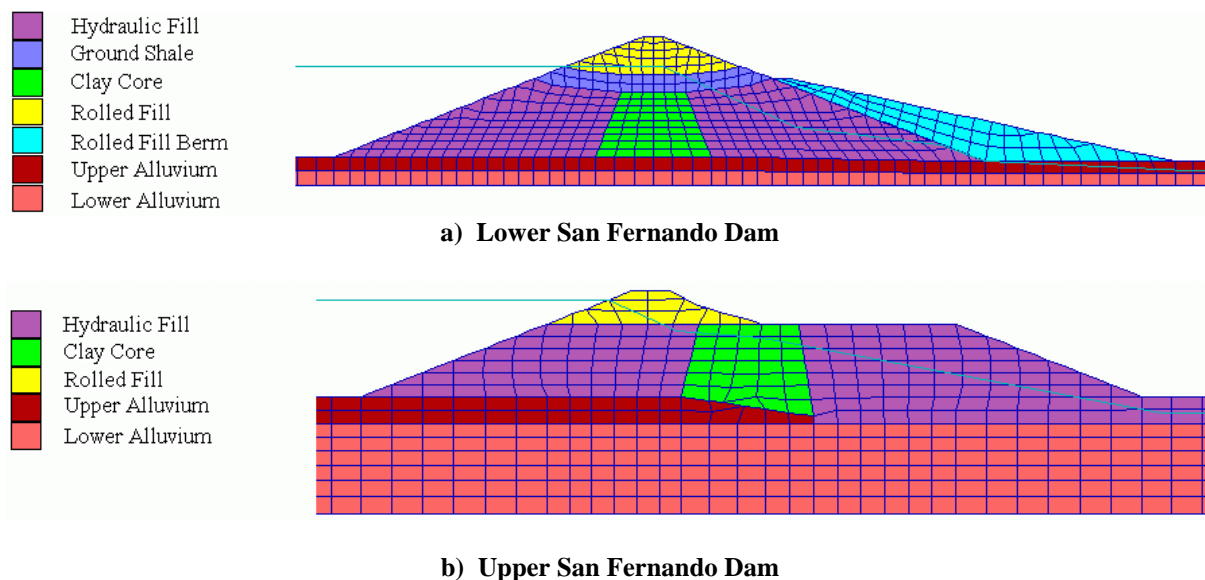
Figure 5: Finite Difference Grids (central portion) and Material Zones

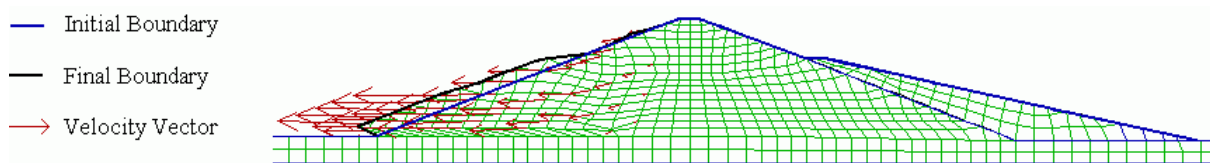**Table 1: Selected Input Properties for Critical Hydraulic Fill Zones**

	Lower San Fernando Dam		Upper San Fernando Dam	Notes
	Upstream	Downstream		
Pre-Liquefaction				
$(N_1)_{60}$	11.5	12.5	13	
$(N_1)_{60-cs}$	13	14	14.5	Corrected for Triggering
$K_{2\,max}$	43	43	30	$G_{max} = C \times K_{2\,max} \times (\sigma'_m)^{0.5}$
MRF	0.14	0.14	0.15	$MRF = (G / G_{max})$
S_u	$\approx$ Drained Strength	$\approx$ Drained Strength	$\approx$ Drained Strength	
Post-Liquefaction				
$(N_1)_{60-cs}$	13.5	14.5	15	Corrected for S_r
S_r / σ'_{vo} • Simple Shear • Compression	0.13 0.5	0.15 0.5	0.16 0.5	
Shear Modulus • $G_{loading}$ • $G_{unloading}$	$S_r / 0.05$ $10 \times G_{loading}$	$S_r / 0.05$ $10 \times G_{loading}$	$S_r / 0.05$ $10 \times G_{loading}$	

shows the estimated displacement vectors at the end of the earthquake. Predicted crest displacements are less than 0.2 metres and downstream slope displacements are less than about 0.3 metres. This is generally consistent with expectations. Figure 6a shows fewer liquefied zones than was anticipated, perhaps due to base isolation effects. Liquefaction at the bottom of the upstream shell coincides with observations. The predicted liquefaction near the upstream face was not observed in the field, and likely resulted from the simplifying assumption of $K_\alpha = 1$. Seed used high values of K_α near the slopes in his evaluation [Seed et al., 1973].

The post-earthquake instability may have resulted from excess pore pressure flowing from loose liquefied zones into denser material, or from the formation of water lenses beneath continuous low-permeability layers. This latter possibility was approximately modelled by continuing the analysis after the earthquake motion had stopped. The strength of liquefied material at the base of the upstream and downstream shells was slowly reduced. The analysis proceeded until the grid became highly distorted. The resulting deformations and velocity vectors are shown in Figure 6b. This pattern indicates a substantial and progressing failure of the upstream shell, and relative stability of the downstream shell. This behaviour is extremely complex and difficult to predict using total stress approaches. Proper investigations fall within the domain of effective stress analyses.

Liquefied Elements
■ With Post-Liq Stress Reversal
□ No Post-Liq Stress Reversal

→ Displacement Vector (Max = 1.9 metres)

a) Liquefied Zones and Displacement Vectors at End of Earthquake

— Initial Boundary
— Final Boundary
→ Velocity Vector

b) Displacing Shape from Post-Earthquake Analysis (Mag. 1X)

Figure 6: Analysis Results for Lower San Fernando Dam

Results for Upper San Fernando Dam

Predicted zones of liquefaction are shown in Figure 7. These zones are more extensive than originally estimated by Seed [1973], especially along the upstream face and beneath the downstream slope. The assumption for K_α should influence the predictions in these locations.

The displaced shape is also shown in Figure 7. Most of the embankment has moved in the downstream direction, including the crest. This agrees with post-earthquake observations. The change in the displacement direction, from downstream to upstream, occurs on the upstream face at about the reservoir level. Again, this conforms with the location of longitudinal cracks. A comparison of actual and simulated displacements is shown in Figure 8. The horizontal pattern agrees well with the observations. The vertical displacement pattern was not predicted as well, although the magnitudes are similar. The analysis also predicts a pressure bulge at the downstream toe, as was observed.

Additional analyses were performed to evaluate the importance of various input parameters. Viscous damping, blowcount, and the residual strength in simple shear were found to be critical variables. Results were relatively insensitive to moderate changes in $G_{loading}$, MRF, and the S_u of non-liquefied sand. The relative significance of these variables may be a function of the structure being analyzed.

CONCLUSIONS

A total stress approach is presented which simulates the pre- and post-liquefaction behaviour of sand. The model permits simultaneous evaluation of triggering and post-liquefaction displacement. It directly considers the reduced stiffness, strength anisotropy, and occurrence of high pore pressure ($r_u = 100\%$) in liquefied soils. Triggering of liquefaction is evaluated on an element by element basis, permitting zones of liquefaction to develop with loading in a rational manner. The effects of progressive liquefaction, including base isolation and load shedding, are directly considered.

The response of the Lower and Upper San Fernando dams to the 1971 San Fernando earthquake was simulated using the method. Reasonable to good agreement was obtained between field observations and the analyses.
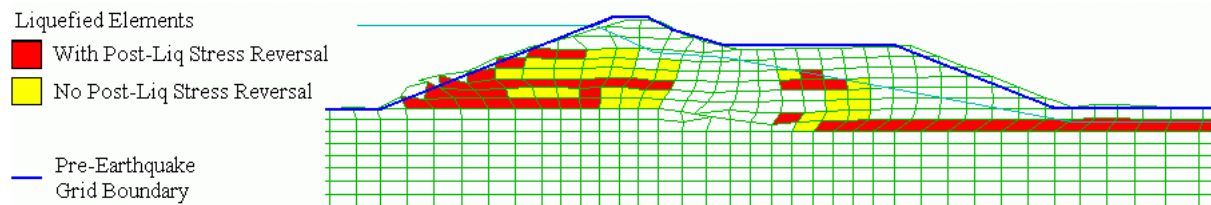

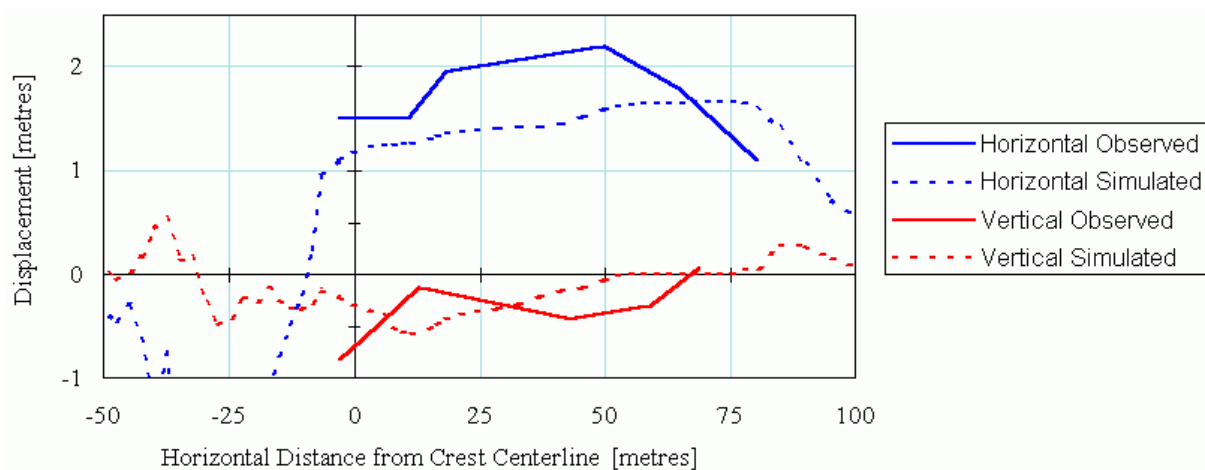**Figure 7: Upper San Fernando Dam — Deformed Shape (Mag. 2X) and Liquefied Zones**

Figure 8: Upper San Fernando Dam — Comparison of Surface Displacements

Critical input parameters include $(N_1)_{60-cs}$, residual strength in simple shear, viscous damping coefficients, direction of loading, and frequency content of the input motion. The highly non-linear nature of the analysis necessitates some level of sensitivity study whenever the approach is used.

The synthesized approach is a powerful and useful analytic tool, but it retains the inherent limitations of a total stress approach. Effective stress analyses are required to properly investigate complex behaviour, such as was observed at the Lower San Fernando dam.

REFERENCES

Bartlett, S.F. and Youd, T.L. (1995), "Empirical Prediction of Liquefaction-Induced Lateral Spread", *Journal of Geotechechnical Engineering*, ASCE, Vol. 121, No. 4, pp316-329.

Beaty, M.and Byrne, P.M. (1998), "An Effective Stress Model for Predicting Liquefaction Behavior of Sand", *Geotechnical Earthquake Engineering and Soil Dynamics III*, ASCE, Vol. 1, pp766 - 777.

Beaty, M.H. and Byrne, P.M. (1999), "Predicting Liquefaction Displacements with Application to Field Experience", *Proceedings 8th Canadian Conference on Earthquake Engineering*, Vancouver, pp335-340.

Byrne, P.M. and Beaty, M.H. (1999), "Assessment of Residual Strength for Embankments*" Proceedings 2nd International Conference on Earthquake Geotechnical Engineering*, Lisbon, Portugal, Balkema, in press.

Finn, W.D.L., Yogendrakumar, M. and Yoshida, N. (1986), "Response of 2D embankment systems to seismic loading – program TARA-3", Soil Mechanics Series, Univ. of British Columbia, Canada.

Harder, L.F., Hammond, W.D., Driller, M.W. and Hollister, N. (1989), *The August 1, 1975 Oroville Earthquake Investigation, Supp. to Bull. 203-78*, Bulletin 203-88, State of California, Dept. of Water Resources.

Idriss, I.M. and Sun, J. (1992), *User's Manual for SHAKE91*, Center for Geotechnical Modeling, UC Davis.

Itasca, (1998), *FLAC, Fast Lagrangian Analysis of Continua, Version 3.40 User's Guide*, Itasca Consulting Group, Inc., Thrasher Square East, 708 South Third Street, Suite 310, Minneapolis, Minnesota.

Lee, K.L. and Chan, K. (1972), "Number of Equivalent Significant Cycles in Strong Motion Earthquakes", *Proc. of the Intern. Conf. on Microzonation for Safer Construction Research and Application*, Vol. 2, pp609-627.

Newmark, N.M. (1965), "Effects of Earthquakes on Dams and Embankments", *Geotechnique*, 15, 2, pp139-160.

Seed, H.B., Lee, K.L., Idriss, I.M. and Makdisi, F. (1973), *Analysis of the Slides in the San Fernando Dams during the Earthquake of Feb. 9, 1971*, Report No. EERC 73-2, EERC and UC Berkeley.

Seed, H.B., Seed, R.B., Harder, L.F., and Jong, H.-L. (1988), *Re-evaluation of the Slide in the Lower San Fernando Dam in the Earthquake of Feb. 9, 1971*, Report No. UCB/EERC-88/04, EERC and UC Berkeley.

Serff, N., Seed, H.B., Makdisi, F.I. and Chang, C.-Y. (1976), *Earthquake Induced Deformations of Earth Dams*, Report No. EERC 76-4, EERC and UC Berkeley.

Vaid, Y.P. and Sivathayalan, S. (1999), "Fundamental factors affecting liquefaction susceptibility of sands", *Proceedings of the International Workshop, Physics and Mechanics of Soil Liquefaction,* Baltimore, Balkema.

Youd, T.L. and Idriss, I.M. (1998), *Proc. of the NCEER Workshop on Evaluation of Liquefaction Resistance of Soils*, Report No. NCEER-97-0022, Multidisciplinary Center for Earthquake Engineering Research.